DOI: 10.1021/ma900312a

Macromolecules
ARTICLE

Synthesis, Optical Properties, and Microstructure of a Fullerene-Terminated Poly(3-hexylthiophene)

Bryan W. Boudouris,[†] Francesc Molins,[‡] David A. Blank,[‡] C. Daniel Frisbie,*[,†] and Marc A. Hillmyer*[,‡]

[†]*Department of Chemical Engineering and Materials Science and* [‡]*Department of Chemistry, University of Minnesota, Minneapolis, Minnesota 55455*

Received February 11, 2009; Revised Manuscript Received April 21, 2009

ABSTRACT: End-functionalized, regioregular poly(3-hexylthiophene) (P3HT) was synthesized by a combination of a controlled polymerization technique and postpolymerization functionalization. Both ends of the polymer chains were terminated with fullerene units to create an internal electron accepting−donating−accepting molecule, methylfulleropyrrolidine−poly(3-hexylthiophene)−methylfulleropyrrolidine (C_{60}-P3HT-C_{60}). The molecular properties of the polymer were characterized using ^{1}H NMR spectroscopy, size exclusion chromatography (SEC), ultraviolet−visible (UV−vis) absorption spectroscopy, and fluorescence spectroscopy. These results show that the fullerene units are covalently bound to the polymer chain ends. Differential scanning calorimetry (DSC), wide-angle X-ray scattering (WAXS), and small-angle X-ray scattering (SAXS) were used to determine the bulk microstructure of the polymers. In addition, atomic force microscopy (AFM) was used to examine spun-cast thin films. These experiments revealed that microphase separation occurs between the main polymer chain and the fullerene end groups and suggests the creation of two distinct semicrystalline regimes in C_{60}-P3HT-C_{60} that are similar to those seen in a compositionally similar blend of P3HT and C_{60}. This comparable domain formation, coupled with the possibility of enhanced charge transfer associated with an internal donor−acceptor material, makes C_{60}-P3HT-C_{60} a promising candidate as a material in bulk heterojunction organic photovoltaics.

Introduction

The search for an economical and flexible supplement to current inorganic solar cells has led to an increased interest in the development of organic photovoltaics (OPVs).[1−3] However, implementation of plastic solar cells has been thwarted by the relatively low efficiency of the devices, currently ∼5% in the best cases.[4,5] To facilitate electron−hole separation, the most efficient organic devices contain two types of semiconductors: an electron donor and an electron acceptor. Regioregular poly(3-hexylthiophene)[6,7] (P3HT) has become the predominant electron-donating material used in polymer-based OPVs because of its high hole mobility (∼0.1−1 $cm^2\ V^{-1}\ s^{-1}$), relatively low band gap (∼1.9 eV), and solution processability.[8−11] In bulk heterojunction systems, P3HT and an electron-accepting soluble fullerene derivative, [6,6]-phenyl-C_{61}-butyric acid methyl ester (PCBM), are solution blended to form an active layer in the most efficient polymer-based OPVs.[12−15] Two key criteria enhance the performance of these devices relative to other polymer-based solar cells due to the seemingly serendipitous relationship between P3HT and PCBM. First, large interfacial area and intimate contact between the fullerene and polymer phases occurs and allows for ultrafast charge separation at the donor−acceptor interface. Second, the materials phase separate in such a way that percolating networks form and allow for charge collection at the appropriate electrodes.[5,16−20] This critical phase separation is currently controlled through a combination of well-tuned spin-coating conditions and thermal annealing treatments in the binary system.[4,5,12,13,16]

Phase separation in single-component systems of block copolymer thin films, on the other hand, has been shown to spontaneously form ∼10 nm domains.[21−23] In addition to providing a pathway for intramolecular charge separation, an electron acceptor−donor−acceptor triblock copolymer affords the possibility of nanodomains formed by the microphase separation of the electron donor and the electron acceptor without the need for additional processing steps. The phase separation observed in these block copolymers could be controlled by varying the length of the constituent chains, allowing for a systematic study of charge transport behavior as a function of domain spacing.

In fact, donor−acceptor molecules previously have been synthesized using fullerene-containing hybrid moieties for application in OPV devices both as charge transport materials and as compatibilizers to enhance active layer morphology.[24−37] Particularly, some oligothiophene and oligo(*p*-phenylenevinylene) systems with fullerene end groups have been synthesized for the purpose of examining their photophysics. While some of these materials have also been used in photovoltaics,[28,29,32] the device efficiencies have so far been low, perhaps due to poor morphologies. Polymeric donor molecules with fullerene end groups, which may potentially form better films, have so far not been extensively researched.

Here we report the synthesis of a difunctional, fullerene-terminated regioregular poly(3-hexylthiophene), methylfulleropyrrolidine−poly(3-hexylthiophene)−methylfulleropyrrolidine (C_{60}-P3HT-C_{60}), through the use of a controlled polymerization and subsequent postpolymerization functionalization. The molecular properties of the polymer were characterized using ^{1}H NMR spectroscopy, size exclusion chromatography (SEC), ultraviolet−visible (UV−vis) absorption spectroscopy, and fluorescence spectroscopy. Differential scanning calorimetry (DSC), wide-angle X-ray scattering (WAXS), small-angle X-ray scattering (SAXS), and atomic force microscopy (AFM) experiments show that this material microphase separates on the nanometer length scale. The size of the P3HT crystallite lamellae, thought to be chiefly responsible for hole transport, are scarcely

*To whom correspondence should be addressed. E-mail: frisbie@cems.umn.edu (C.D.F.); hillmyer@umn.edu (M.A.H.).

 Published on Web 05/21/2009

affected by the inclusion of the relatively bulky end groups on the polymer. In addition, the fullerene units on the polymer chain aggregate into domains with a crystal packing that is similar to that observed for powders of a related small molecule, *N*-methylfulleropyrrolidine (NMC_{60}). The C_{60}-P3HT-C_{60} polymer also has a similar X-ray scattering pattern to that of a binary blend of P3HT and C_{60} (mixed in approximately the same weight ratio as that contained in C_{60}-P3HT-C_{60}) but with the added advantage of having the electron donor and acceptor covalently bound.

We believe that this system offers an advantage over previously studied oligothiophene−fullerene systems due to the synthetic simplicity of this molecule. The P3HT polymerization technique utilized in this work is much less labor-intensive than the stepwise routes used to grow oligothiophenes and also allows for the easy manipulation of the average number of repeat units in the chains by varying reaction conditions. The crystallization-induced phase separation of C_{60}-P3HT-C_{60} is likely to result in interesting and potentially useful morphologies. This opens up possibilities for systematic studies of OPV cells based on C_{60}-P3HT-C_{60} where the molecular weight of the P3HT block is tuned. In addition, we plan a thorough examination of the photophysics and exciton dissociation of C_{60}-P3HT-C_{60} in a solvent which will yield insight into exciton diffusion lengths in the long-chain cases. These points are the motivation for studying this new, macromolecular fullerene−polythiophene−fullerene system.

Experimental Section

General Methods. The ^{1}H NMR spectra were measured on a Varian VI-500 spectrometer using deuterated chloroform (Cambridge) solutions containing ~1 wt % polymer. Elemental analysis was performed by Micro-Analysis, Inc., Wilmington, DE (see Supporting Information). As expected, the percentage of carbon and nitrogen was higher in C_{60}-P3HT-C_{60} than in P3HT; however, quantitative agreement between the calculated and measured composition was not observed. Quantitative analysis of fullerene-containing species is hampered by the incomplete combustion of fullerene and retention of residual solvent.[38−40] Analytical size exclusion chromatography (SEC) data were collected on an Agilent 1100 series equipped with an Agilent ultraviolet−visible (UV−vis) light detector (path length = 10 mm) and three PLgel 5 μm MIXED-C columns. For the molecular weight and polydispersity characterizations, chloroform at 35 °C was used as the mobile phase at a flow rate of 1 mL/min, and the SEC data were calibrated with polystyrene standards and known Mark−Houwink parameters for poly(3-hexylthiophene) and polystyrene (Polymer Laboratories).[41,42] Measurements using the UV−vis signal of the SEC spectra used chloroform at room temperature as the mobile phase at a flow rate of 1 mL/min. Preparatory size exclusion chromatography (prep SEC) was performed on an Agilent 1100 series equipped with an Agilent UV−vis light detector (path length = 10 mm) and two PLgel 10 μm MIXED-D columns. Chloroform at 35 °C was used as the mobile phase at a flow rate of 6 mL/min as to keep the internal pressure of the columns approximately equal to the pressure used during analytical SEC experiments. Matrix-assisted laser desorption/ionization-mass spectroscopy (MALDI-MS) measurements were performed on a Bruker Reflex III operating in linear mode. A typical sample was prepared by mixing 5 μL of a polymer solution in THF (5 mg/mL) and 15 μL of a dithranol solution in THF (20 mg/mL). The mixture (~1 μL) was then spotted onto the plate. Cytochrome *c* (Bruker) was used externally for calibration.

Spectroscopic Characterization. Molar absorption coefficients were calculated using static ultraviolet−visible (UV−vis) absorption spectra of polymer (dissolved in chloroform) solutions and were taken on a Spectronic Genesys 5 spectrometer over a wavelength range of 200−900 nm using a chloroform-containing quartz cuvette (Starna Cells, Inc.) with a 10 mm path length as a blank. Thin films for absorbance measurements were made by spin-coating polymer solution in 1,2-dichlorobenzene (10 mg/1 mL) onto glass substrates at 600 rpm for 1 min. The films were then allowed to dry slowly in a covered Petri dish in an inert atmosphere glovebox.[4] Film thicknesses were estimated by scratching the polymer film and measuring the step change with a KLA-Tencor P16 profilometer. The thickness of the P3HT film was 69 ± 3 nm, and the thickness of the C_{60}-P3HT-C_{60} film was 52 ± 3 nm. Fluorescence data were acquired on a FluoroLog 2 fluorimeter (SPEX) with solutions of the polymers in either chloroform or toluene. A binary mixture of P3HT and [6,6]-phenyl-C_{61}-butyric acid methyl ester (PCBM) was made by dissolving the two materials with the ratio of 2.1 mol equiv of free PCBM for every polymer chain in solutions (P3HT + PCBM). The samples were prepared to obtain an optical density 0.1−0.3 for C_{60}-P3HT-C_{60} and 0.1−0.2 for the P3HT and the P3HT + PCBM samples. Solutions of Coumarin 153 (Exciton) in MeOH were used as the quantum yield (QY) standards and had a known value of 0.42.[43] The fluorescence intensity of the polymer samples and the standard were independent of purging with inert gas so no precautions with regard to air were taken in these measurements. Fluorescence spectra of the polymers and standard, with an excitation wavelength of 440 nm, were collected back to back and corrected for frequency-dependent detector sensitivity.

Thermal and Structural Characterization. Differential scanning calorimetry (DSC) measurements were acquired using a TA Q1000 calorimeter. The samples were first annealed at 260 °C and then cooled to −60 °C at a rate of 10 °C/min. The results shown are for the final sample heating at a rate of 10 °C/min. An indium standard was used to calibrate the instrument, and nitrogen was used as the purge gas. Wide-angle X-ray scattering (WAXS) data were collected in the diffraction angular range of $3° \leq 2\theta \leq 31°$ by a Bruker-AXS D5005 microdiffractometer. The crystalline peaks were deconvoluted using the curve-fitting software, JADE 8 (CMI). Small-angle X-ray scattering (SAXS) measurements were made on a home-built beamline at the University of Minnesota and used copper Kα radiation (λ = 1.54 Å) as the X-ray source. All data were corrected for detector response characteristics. Atomic force microscopy (AFM) images were taken with a Veeco Metrology (previously Digital Instruments) Nanoscope IIIa Multimode microscope operating in tapping mode in the repulsive regime under inert atmosphere. The probe tips were fabricated by Mikromasch USA (NSC15/AlBS tips, resonant frequency 265−400 kHz, and spring constant 40 N/m).

Blending of P3HT/C_{60} Mixture. In order to make a binary blend of P3HT and C_{60} in approximately the same weight ratio as that of the C_{60}-P3HT-C_{60} polymer, 30 mg of P3HT and 8 mg of C_{60} were dissolved in 10 mL of chloroform. This led to a blend with a 0.21 weight fraction of C_{60} ($w_{C_{60}}$ = 0.12). The solution was allowed to stir at room temperature until the mixture was completely dissolved. At this point the solution was drop-cast into a tin pan and allowed to dry. The mixture (P3HT/C_{60} mixture) was recovered from the pan and dried overnight under vacuum.

P3HT and C_{60}-P3HT-C_{60} Thin Film Preparation. Solutions of P3HT and C_{60}-P3HT-C_{60} were made by dissolving 3 mg of polymer in 1 mL of 1,2-dichlorobenzne (DCB) and allowing the solutions to stir at 60 °C under an inert atmosphere overnight. Silicon wafers with a 3000 Å thermally grown silicon oxide layer were used as the substrates for the films. Solutions were passed through a 0.45 μm syringe filter, and the solutions were deposited on the substrates. The rotation rate was then increased from 0 to 2000 rpm over the course of ~5 s and held at 2000 rpm for 60 s inside an inert atmosphere glovebox. The films were then annealed in inert atmosphere for 10 min at 150 °C.

Results and Discussion

Synthesis of C_{60}-P3HT-C_{60}. Regioregular poly(3-hexylthiophene) was synthesized using the controlled Grignard

Scheme 1. Synthesis of Methylfulleropyrrolidine−Poly-(3-hexylthiophene)−Methylfulleropyrrolidine (C_{60}-P3HT-C_{60})

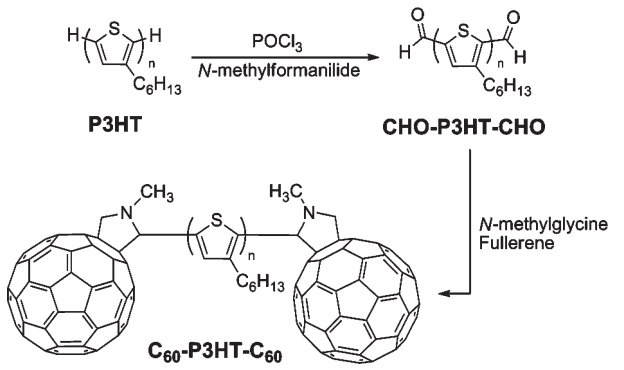

Metathesis (GRIM) polymerization method and yielded P3HT with a narrow molecular weight distribution (M_w/M_n = 1.3).[44] To remove any small molecular weight impurities residual in the reaction mixture,[45] the polymer was purified using a Soxhlet extraction apparatus with methanol, acetone, and chloroform in a sequential manner. The chloroform fraction was then used in the subsequent reactions. The P3HT was initially designed to have a lower molecular weight to aid in molecular characterization. Our experience with higher molecular weight P3HT derivatives suggests that the influence of chain length on the end group reactivity is not a significant concern. The utility of end-functionalized P3HTs has previously been shown in the synthesis of polythiophene-containing block copolymers,[46−48] and the postpolymerization functionalization route for the synthesis of C_{60}-P3HT-C_{60} is shown in Scheme 1.

After converting the bromine−hydrogen end-capped polymer (H-P3HT-Br) to the proton-terminated polymer (P3HT) by use of a magnesium−halogen reaction,[49] the P3HT was converted to the bis-aldehyde-terminated molecule (CHO-P3HT-CHO) in a Vilsmeier−Haack reaction with phosphorus oxychloride and *N*-methylformanilide used in excess.[50] Finally, the polymer was converted to the desired product, methylfulleropyrrolidine−poly(3-hexylthiophene)−methylfulleropyrrolidine (C_{60}-P3HT-C_{60}), by using an excess of *N*-methylglycine and fullerene to drive the 1,3-dipolar cylcoaddition (Prato) reaction to completion as in analogous reactions previously shown in the literature for small molecules.[24−30,51] Preparatory size exclusion chromatography (prep SEC) was utilized to separate the polymer from the excess fullerene. Figure S1 shows a representative prep SEC chromatogram of the separation procedure illustrating the large retention time difference between the elution of the C_{60}-P3HT-C_{60} and unreacted fullerene making for the facile collection of only the polymer. The polymer was collected from the elution times (t_{elute}) of 22 min < t_{elute} < 33 min.[52]

Molecular Structure of C_{60}-P3HT-C_{60}. To determine the molecular weight distribution of the polymers, analytical size exclusion chromatography (SEC) was performed on the macromolecules with a UV−vis detector that was also capable of collecting the UV−vis spectrum of the polymer as the material eluted through the column over the absorption range of both P3HT and C_{60}. The molecular weight distribution of the P3HT did not change during the Vilsmeier reaction step in generating CHO-P3HT-CHO. However, there is a significant amount of coupling that occurs during the addition of fullerene to the end of the polymer chains and is reflected by the second peak on the SEC trace shown in Figure 1a. The coupling caused the molecular weight to increase from $M_n \sim 5400$ g mol^{-1} to $M_n \sim 7600$ g mol^{-1}

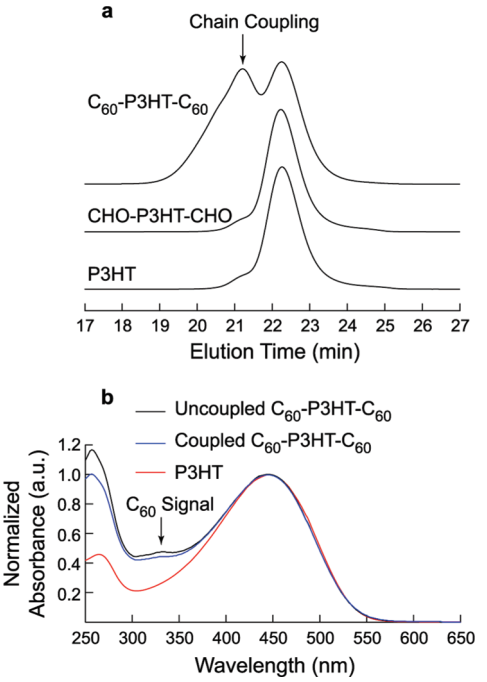

Figure 1. (a) SEC chromatograms of C_{60}-P3HT-C_{60} and the polymer precursors with chloroform as the eluting solvent at 35 °C. The traces were obtained using a UV−vis detector monitoring the signal at λ = 400 nm. The traces are offset vertically for clarity. (b) The online UV−vis spectra at room temperature for the P3HT precursor and C_{60}-P3HT-C_{60} in chloroform at the two maxima in the SEC plots for the coupled polymer (t_{elute} = 21.2 min) and uncoupled polymer (t_{elute} = 22.3 min).

(41% increase) and for the molecular weight distribution to increase from $M_w/M_n \sim 1.3$ to $M_w/M_n \sim 1.8$ as measured by SEC against polystyrene standards and with the data corrected using published Mark−Houwink parameters.[41,42] The increase in molecular weight is also reflected in the ^{1}H NMR measurements with integration of the polymer end groups showing an increase from $M_n \sim 4500$ g mol^{-1} for CHO-P3HT-CHO to $M_n \sim 6700$ g mol^{-1} for C_{60}-P3HT-C_{60} (48% increase). Control reactions run at similar conditions to the Prato reaction without the fullerene present showed that chain coupling was still a major problem in the reaction process. However, simply refluxing chlorobenzene with P3HT dissolved in solution does not lead to chain coupling. This suggests that the macromolecular azomethine ylide intermediate generated in situ from the reaction of CHO-P3HT-CHO and *N*-methylglycine is required for the coupling of the polymer chains. While previous reports of the dimerization of thiocarbonyl[53] and thiophenedicarboxaldehyde-containing[54] ylide intermediates imply a possible mechanism for this coupling, further experiments are required to confirm this observation. Despite the chain coupling that occurs during the C_{60} addition step, the UV−vis absorption spectra obtained at the two peaks (t_{elute} = 21.2 min and t_{elute} = 22.3 min) in the C_{60}-P3HT-C_{60} SEC chromatogram shown in Figure 1b agree with ^{1}H NMR spectroscopy (see below) and suggest that every polymer chain has both ends terminated with fullerene. The uncoupled C_{60}-P3HT-C_{60} polymer chains show a more pronounced fullerene absorption signal at λ = 330 nm than the coupled C_{60}-P3HT-C_{60} polymer chains since the fullerene is now a larger percent of the composition of the uncoupled chains. In addition, it is apparent that the unreacted fullerene is no longer present in the C_{60}-P3HT-C_{60} sample as depicted in the full SEC traces shown in Figure S2.

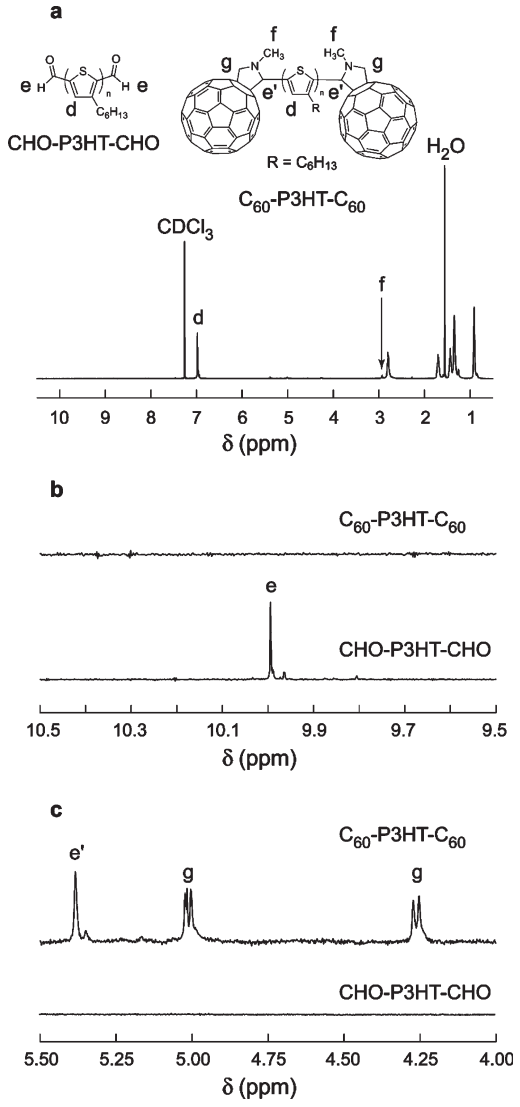

Figure 2. ^{1}H NMR spectra of (a) C_{60}-P3HT-C_{60}, (b) the region near $\delta = 10$ ppm showing the disappearance of the aldehyde proton signal upon addition of fullerene, and (c) the region near $\delta = 5$ ppm showing the appearance of the signals related to the fullerene end groups. The unlabeled peaks upfield of $\delta = 5$ ppm in (a) are from the alkyl group protons. All polymers were dissolved in deuterated chloroform, and spectra were recorded at room temperature. The coupling constant of the resonance at $\delta \sim 4.3$ ppm is $J = 9.5$ Hz, and the coupling constant of the resonance at $\delta \sim 5.0$ ppm is $J = 10$ Hz.

The conversion of end groups during the postpolymerization functionalization was monitored using ^{1}H NMR spectroscopy, matrix-assisted laser desorption/ionization-mass spectroscopy (MALDI-MS), and ultraviolet−visible (UV−vis) light spectroscopy. The molecular weights of the P3HT polymers were determined by ^{1}H NMR spectroscopy using end-group analysis, and these molecular weights were used in all further computations. While calculations were based on NMR-determined molecular weights, Mark−Houwink corrected SEC molecular weights were similar to those (<6 repeat units difference) determined by end-group integrations. The molecular structures of CHO-P3HT-CHO and C_{60}-P3HT-C_{60} along with the ^{1}H NMR spectrum of C_{60}-P3HT-C_{60} are shown in Figure 2. Parts b and c of Figure 2 show the relevant ^{1}H NMR spectra regimes for the end groups of CHO-P3HT-CHO and C_{60}-P3HT-C_{60}, respectively. End-group integration showed complete conversion of the aldehyde-terminated polymer to the fullerene-terminated polymer. The peaks around $\delta \sim 10$ ppm in the CHO-P3HT-CHO spectrum are due to the substitution of the aldehyde group at either the 2-position of the terminal thiophene ring (higher intensity) or the 5-position of the thiophene ring (lower intensity).[49] This is also reflected in the C_{60}-P3HT-C_{60} spectrum as the e′ protons show two resonances with a small difference in chemical shift. The chemical shifts and splitting patterns of the end groups were also in agreement with previous reports[24,28] with the protons labeled e′ and g having integrations of 2:2:2. Note that the protons labeled g are diastereotopic due to the adjacent stereocenter. The coupling constant of the resonance at $\delta \sim 5.0$ ppm is $J = 9.5$ Hz, and the coupling constant of the resonance at $\delta \sim 4.2$ ppm is $J = 10$ Hz, which is consistent with reported literature values for small molecule systems.[24]

Matrix-assisted laser desorption/ionization-mass spectrometry (MALDI-MS) measurements were also performed to verify the end-group functionality of C_{60}-P3HT-C_{60}. Two major sets of peaks were observed with the first type associated with C_{60}-P3HT-C_{60}. As observed in other fullerene-capped systems,[55−57] the second major set corresponds to P3HT moieties where both fullerene units have fragmented from the polymer chain during the desorption/ionization process to yield species with m/z = [C_{60}-P3HT-C_{60}] − 1440 (Figure S3).

To verify the amount of fullerene end groups per polymer chain determined by ^{1}H NMR spectroscopy, absorbance at selected wavelengths versus concentration of species plots were constructed to determine the molar absorption coefficient of P3HT and C_{60}. These molar absorption coefficients were found using the slope of the linear fits shown in Figure 3b,c for wavelengths of $\lambda = 330$ nm in the fullerene system and $\lambda = 330$ and 448 nm in the P3HT system. The molar absorption coefficients were found to be $\varepsilon_{330} = 5.3 \times 10^4$ M^{-1} cm^{-1} for fullerene and $\varepsilon_{330} = 5.5 \times 10^4$ M^{-1} cm^{-1} and $\varepsilon_{448} = 20 \times 10^4$ M^{-1} cm^{-1} for P3HT. From this point a system of linear equations involving two variables and two unknowns was solved using the Beer−Lambert law. Because the connection between the donor and acceptor contained one nonconjugated bond, the molar absorption coefficients are likely not significantly affected by covalent attachment.[58]

$$A_{330}^{\text{total}} = A_{330}^{\text{P3HT}} + A_{330}^{\text{C}_{60}} = \varepsilon_{330}^{\text{P3HT}} b[\text{P3HT}]_{330} + \varepsilon_{330}^{\text{C}_{60}} b[\text{C}_{60}]_{330} \quad (1)$$

$$A_{448}^{\text{total}} = A_{448}^{\text{P3HT}} + A_{448}^{\text{C}_{60}} = \varepsilon_{448}^{\text{P3HT}} b[\text{P3HT}]_{448} + \varepsilon_{448}^{\text{C}_{60}} b[\text{C}_{60}]_{448} \approx \varepsilon_{448}^{\text{P3HT}} b[\text{P3HT}]_{448} \quad (2)$$

In these equations, A_i is the total absorbance of the polymer at wavelength i at room temperature from the solution spectra shown in Figure 3a, b is the path length of the detection cell (10 mm), and [X] is the concentration of species X. Equation 2 becomes simplified because the absorbance of fullerene at $\lambda = 448$ nm is approximately zero. Using the NMR-determined molecular weight ($M_n \sim 6700$ g mol^{-1}) for the main chain of the polymer (this includes the coupled and uncoupled chains) and 1552 g mol^{-1} for the molecular weight of methylfulleropyrrolidine end groups, we find the theoretical weight fraction of the fullerene end groups is $w_{C_{60}} = 0.19$ for C_{60}-P3HT-C_{60}. Solving for the actual composition using eqs 1 and 2 yields a value of $w_{C_{60}} = 0.14$ for the fullerene-capped polymer, in reasonable agreement with the predicted value. Utilizing the two equations above and the raw data obtained prior to normalization of the plots shown in Figure 3b, we find that the UV−vis data indicate the fullerene end-functionalization is slightly lower than the ^{1}H NMR spectroscopy data suggests but the results are in relatively good agreement and

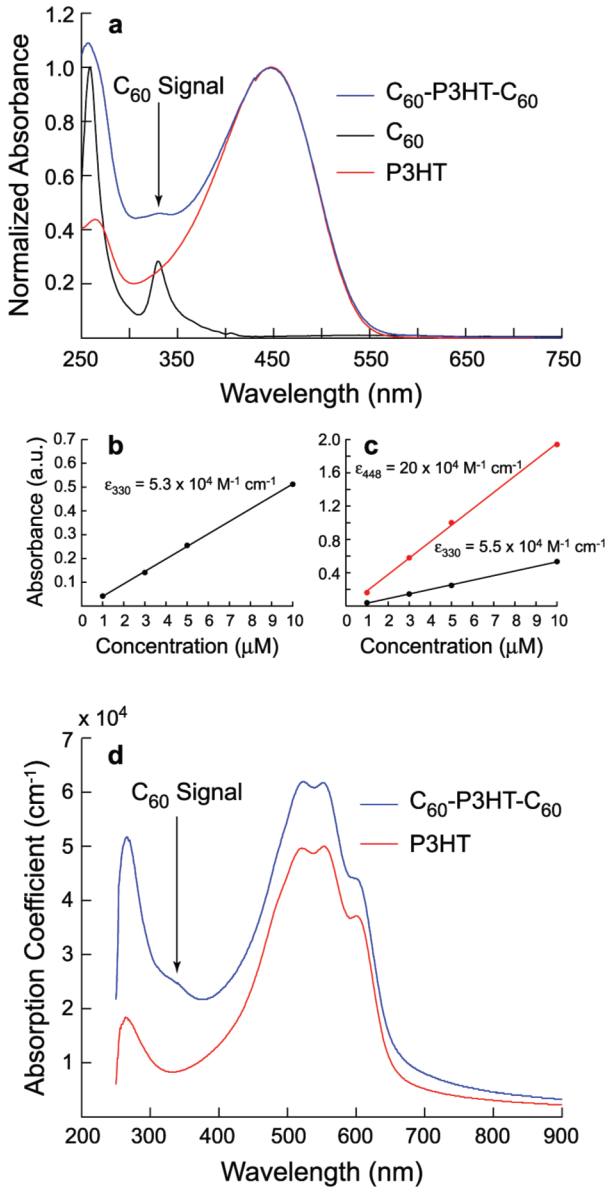

Figure 3. (a) UV−vis absorption data of 5 μM solutions of P3HT, C_{60}, and C_{60}-P3HT-C_{60} in chloroform at room temperature. Absorbance as a function of concentration in chloroform solutions for (b) C_{60} and (c) P3HT at selected wavelengths (λ = 330 nm and λ = 448 nm). (d) UV−vis absorption coefficients for thin films of P3HT (d ~70 nm) and C_{60}-P3HT-C_{60} (d ~52 nm) spun-coat from 1,2-dichlorobenzene solutions.

indicate that the majority of the polymer chains are capped on both ends with fullerene units.

Thin film UV−vis absorbance spectra were also acquired for P3HT and C_{60}-P3HT-C_{60}. As shown in Figure 3d, both spectra exhibit four local maxima over the range of the P3HT absorption; included in these maxima is a shoulder at $\lambda \approx 625$ nm which is associated with vibronic structure and is an indication of crystalline order consistent with the wide-angle X-ray scattering data (see Figure 6). The C_{60}-P3HT-C_{60} spectrum contains a small shoulder at $\lambda \approx 330$ nm, and a significant increase in the thin film absorption relative to P3HT at $\lambda \approx 275$ nm is also present. Both of these observations are consistent with absorption of fullerene species. The absorption coefficients calculated at the maximum absorption wavelength (λ = 552 nm) were $\alpha_{P3HT} = 5.0 \times 10^4$ cm^{-1} and $\alpha_{C_{60}\text{-P3HT-}C_{60}} = 6.2 \times 10^4$ cm^{-1} for the P3HT and C_{60}-P3HT-C_{60} films, respectively.

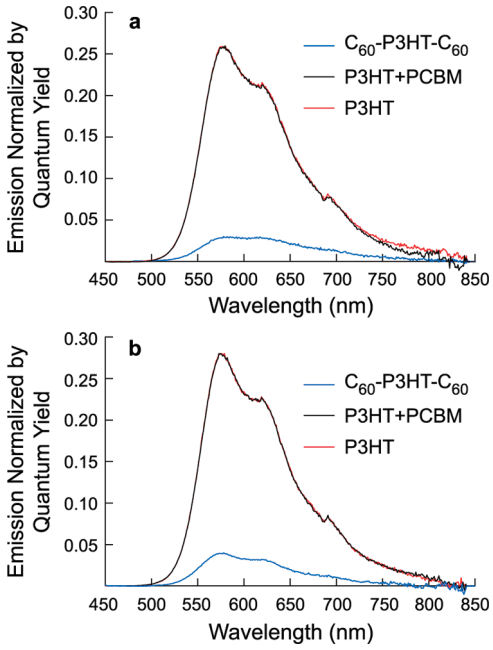

Figure 4. Fluorescence spectra for P3HT, P3HT + PCBM, and C_{60}-P3HT-C_{60} in (a) chloroform and (b) toluene where the emission signal has been normalized by the quantum yield of each of the samples.

Importantly, fluorescence quenching experiments were performed on chloroform solutions of the polymers (Figure 4a). The emission spectra of all polymers show a primary peak and a shoulder at higher wavelengths, which is consistent with previous reports.[28] The calculated quantum yield of the C_{60}-P3HT-C_{60} polymer is 0.03, which is 7 times less than the quantum yields of both P3HT and a mixture of unbound P3HT and PCBM (P3HT + PCBM) where 2.1 equiv of free PCBM was added to the solution for every polymer chain. The highly soluble fullerene derivative PCBM was used in place of C_{60} to ensure that the quencher was dissolved in solution with P3HT. Figure 4b shows fluorescence quenching measurements of the same three samples dissolved in toluene. Significant quenching is once again seen in the C_{60}-P3HT-C_{60} molecule relative to the other systems. Previous studies have shown that when quenching occurs in a similar manner in both chloroform and toluene that energy transfer is the likely means of relaxation;[27,28,59−61] however, ultrafast spectroscopy measurements are required to confirm that electron transfer does not account for at least a fraction of the quenching in the chloroform system.

We have concluded that the polymer C_{60}-P3HT-C_{60} is a mixture of two types of polymer chains and contains a bimodal distribution of these chains with the majority of all types of polymer chains terminated on both ends with fullerene groups. The distribution of the uncoupled polymer chains is the same as the CHO-P3HT-CHO starting material. The size distribution of these molecules is centered about 27 thiophene repeat units per polymer chain, and this type of polymer chain composes 52% of the bimodal mixture by weight. The coupled P3HT chains contain an ill-defined linkage along the backbone of the polythiophene chain and have a distribution twice the length of the uncoupled chains on average. This average is centered on 54 thiophene repeat units per polymer chain, and the coupled chains compose the remainder (48% by weight) of the bimodal mixture. We are confident that the UV−vis spectroscopic signals (and the subsequent X-ray diffraction pattern reflections) associated with fullerene can be attributed to the *end groups of the*

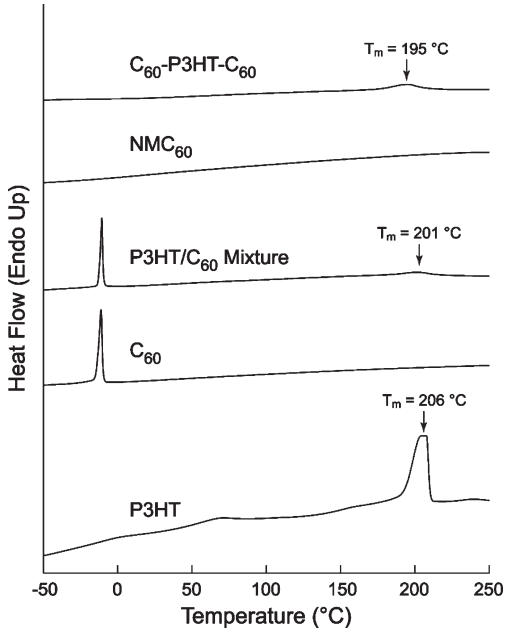

Figure 5. DSC thermograms of P3HT, C_{60}, the P3HT/C_{60} mixture, NMC_{60}, and C_{60}-P3HT-C_{60}. The scans shown were collected at a heating rate of 10 °C/min after annealing at 260 °C and then cooling to −60 °C. The arrows mark the P3HT main-chain melting temperature of the applicable samples. The percent crystallinity of the polythiophene components (see text for details) of P3HT and C_{60}-P3HT-C_{60} were 11% and 10%, respectively.

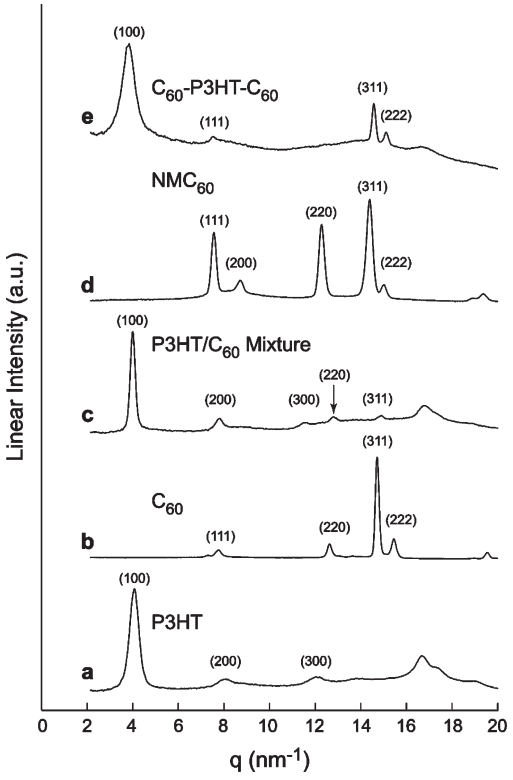

Figure 6. WAXS spectra of (a) P3HT, (b) C_{60}, (c) the P3HT/C_{60} mixture, (d) NMC_{60}, and (e) C_{60}-P3HT-C_{60} obtained at room temperature. The sizes of the polymer crystallites were found to be 13, 14, and 11 nm for P3HT, the P3HT/C_{60} mixture, and C_{60}-P3HT-C_{60}, respectively, using Scherrer's relation. The spectra are offset for clarity.

polymer chain and not due to unreacted, free C_{60} present in what would be a mixture of polymer and small molecule.

Thermal and Microstructural Characterization of C_{60}-P3HT-C_{60}. We used DSC to determine the melting temperatures of the polymer and fullerene samples and to estimate the amount of P3HT crystallinity in the polymers (Figure 5). As previously seen in the literature, C_{60} undergoes a first-order phase transition around −11 °C, and this peak is associated with a crystal rearrangement from a simple cubic structure to a face-centered-cubic crystal packing.[62] The melting transition of C_{60} was not observed in the temperature range scanned. Unlike the parent C_{60} molecule, *N*-methylfulleropyrrolidine (NMC_{60}) does not experience the simple cubic to face-centered-cubic crystal packing transition presumably due to the substituents of NMC_{60}. This molecule also does not exhibit a melting endotherm in the temperature range scanned. As is commonly seen in P3HT, two melting transitions were observed in the H-P3HT-H molecule. The first transition is a broad transition ranging from $T \sim 50$ °C to $T \sim 75$ °C and is associated with the side-chain melting of interdigitated hexyl groups.[63] The main-chain melting of P3HT was found to be at $T \sim 206$ °C. The mixture of P3HT and C_{60} shows both the crystal transition melting temperature associated with the fullerene component and the main-chain melting transition of the polythiophene. Finally, C_{60}-P3HT-C_{60} also exhibits the melting transition of the polythiophene at $T \sim 195$ °C but does not exhibit the simple cubic to face-centered-cubic rearrangement because the molecule present at the end of the polymer chains is more akin to NMC_{60}, which also is incapable of the crystal rearrangement transition. The melting point depressions observed in both the P3HT/C_{60} mixture and C_{60}-P3HT-C_{60} systems are expected because the fullerene acts as an impurity that depresses the freezing (melting) temperature of the semicrystalline polymer.[64] The amount of polymer that was crystalline in the P3HT and C_{60}-P3HT-C_{60} samples was determined by integrating the area under the melting peak in each of the samples, normalizing the values by the amount of P3HT present in the sample, and comparing this with the literature value for the enthalpy of fusion for an ideal P3HT crystal, $\Delta H_m^\infty = 99$ J g^{-1}.[65] The amount of polythiophene that was crystalline in each sample was 11% and 10% for the P3HT and C_{60}-P3HT-C_{60} samples, respectively, which is typical for lower molecular weight P3HTs. Therefore, the bulky end groups of the polymer chain appear to only have a minor impact on the semicrystalline nature of P3HT according to the DSC data.

Wide-Angle X-ray Scattering (WAXS) and Small-Angle X-ray Scattering (SAXS). The spectra in Figure 6 show the WAXS powder scattering patterns of P3HT, C_{60}, the P3HT/C_{60} mixture, NMC_{60}, and C_{60}-P3HT-C_{60}. As is common with P3HT, the first three reflections observed in Figure 6a are the (100), (200), and (300) peaks consistent with a lamellar morphology within the crystalline regions of the polymer and side-group interdigitation.[66] The C_{60} scattering pattern in Figure 6b is also consistent with previously observed results for buckminsterfullerene, which is known to have a face-centered-cubic (fcc) crystal structure at room temperature, and shows reflections for the (111), (220), (311), and (222) indices.[62,67,68] The P3HT/C_{60} mixture spectra is a combination of the individual P3HT and C_{60} single species spectra where the (100), (200), and (300) crystalline reflections of the polythiophene phase are prominent while the (220) and (311) reflections of the fullerene phase are present but are not as accentuated. However, this does suggest that the mixture contains two crystalline domains: one associated with the polythiophene and one associated with the fullerene. Figure 6d shows the reference spectrum of free NMC_{60} and indicates that this molecule has a very similar scattering pattern to that of free C_{60} but with reflections shifted to slightly lower q values (slightly higher domain spacings) due to the substituents present on the NMC_{60} molecule. Also

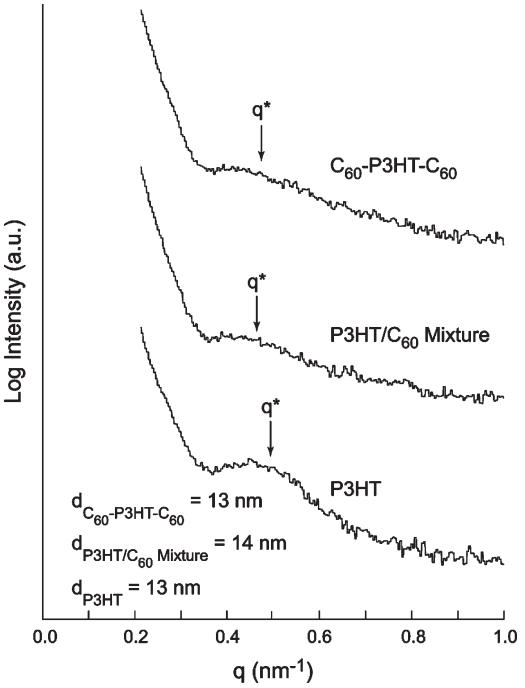

Figure 7. SAXS spectra at 30 °C after annealing at 220 °C for 5 min and slowly cooling to room temperature of P3HT, the P3HT/C_{60} mixture, and C_{60}-P3HT-C_{60}. The principal reflection, q^*, for each sample is marked with an arrow. The corresponding domain spacings calculated from q^* values for the samples are listed at the lower left-hand part of the plot.

present in this sample is the (200) reflection which is allowable for an fcc crystal lattice but not commonly observed in the case of C_{60}.[62,67,68] Much like the P3HT/C_{60} mixture, the C_{60}-P3HT-C_{60} spectra in Figure 6e appears to be a combination of the P3HT and NMC_{60} scattering patterns and suggests the presence of unique polythiophene and fullerene crystalline regimes because of the prescence of both the (100) P3HT peak and the (311) and (222) NMC_{60} reflections. For the three P3HT-containing samples, the average sizes of the polymer crystallites were estimated by using Scherrer's relation.[69] The sizes of the polymer crystallites were found to be 13, 14, and 11 nm for P3HT, the P3HT/C_{60} mixture, and C_{60}-P3HT-C_{60} samples, respectively. These values are similar to those previously seen in the literature for unannealed P3HT samples,[70] and the fact that the crystallite size of the P3HT remains almost unchanged even with the bulky fullerene side groups is noteworthy. We note that peak broadening in WAXS can have other origins besides small crystallite sizes (e.g., inhomogeneous strains). Nevertheless, the formation of discrete domains is consistent with the phase separation seen in other polymer−fullerene systems.[71,72]

In addition to WAXS spectra, SAXS was also employed to observe the domain spacing of P3HT and the C_{60}-P3HT-C_{60} triad. Figure 7 shows the obtained spectra at 30 °C after annealing at 220 °C for 5 min. The presence of weak, broad peaks corresponding to domain spacings of $d \sim 13-14$ nm are consistent with lamellae (nanofibril) widths previously observed in thin films of regioregular P3HT samples cast from selected solvents.[73] In agreement with the WAXS data, the crystallite structure is more prominent in the P3HT sample over both the P3HT/C_{60} mixture and the C_{60}-P3HT-C_{60} triad.

Thin Film Imaging. As polymer thin films are important in the application of OPV devices, atomic force microscopy (AFM) operating in tapping mode was used to acquire

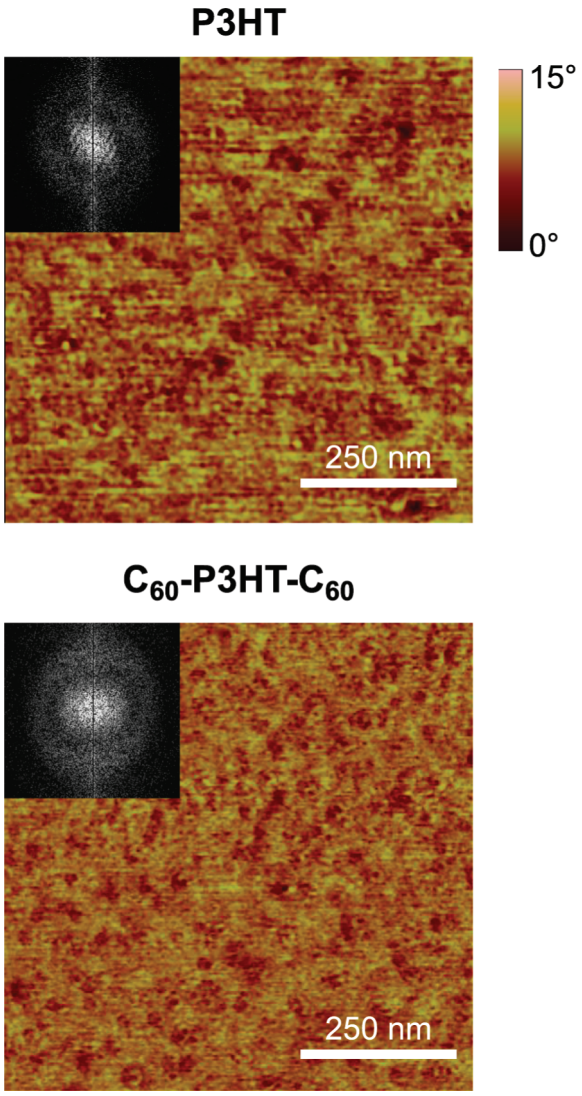

Figure 8. AFM phase images of thin films of P3HT and C_{60}-P3HT-C_{60} and corresponding FFT insets. Processing the FFT data showed characteristic domain dimensions of 14 and 13 nm for P3HT and C_{60}-P3HT-C_{60}, respectively. The films were formed by spin-coating a solution that contained 3 mg of polymer in 1 mL of 1,2-dichlorobenzene at a rotation rate of 2000 rpm for 1 min onto a silicon dioxide substrate. The films were then annealed at 150 °C for 10 min in an inert atmosphere glovebox.

phase images of thin films. The thin films were spun-coat onto thermally grown silicon dioxide from a 3 mg of polymer in 1 mL of 1,2-dichlorobenzene solution. The films were then annealed at 150 °C in an inert atmosphere glovebox for 10 min. The phase images are shown in Figure 8 with the fast Fourier transfer (FFT) data inset in the upper left-hand corners of the images. The films are rather smooth and both have a root-mean-square (rms) roughness of 0.3 nm over the 750 nm scan range shown in Figure 8. While the crystalline P3HT lamellae are not as distinct as shown in previous works,[46,73,74] the integration of the FFT of the films gave characteristic dimensions of 14 and 13 nm for the P3HT and C_{60}-P3HT-C_{60} films, respectively. These numbers compare reasonably well with the dimensions obtained for the nanofibril widths seen in the SAXS spectra (especially considering the inherent error due to the radius of curvature associated with the tip of the AFM cantilever) and previously in the literature, which suggests that the morphologies observed in the bulk are also present in thin films.[73,74]

Conclusions

We have described the synthesis of fullerene end-functionalized regioregular poly(3-hexylthiophene), C_{60}-P3HT-C_{60}. We find that the final step in the reaction sequence leads to chain coupling and speculate that this occurs through an azomethine ylide intermediate which causes a slight increase in the overall molecular weight and a larger increase in the polydispersity of the poly(3-hexylthiophene). The molecules were characterized using a variety of techniques to ensure that the majority of the polymers (including both the coupled and uncoupled polymer chains) contained covalently bound fullerene and no free C_{60}. Thermal characterization reveals that C_{60}-P3HT-C_{60} does experience a melting transition at a slightly depressed temperature from that observed in P3HT presumably due to packing frustration brought about by the relatively bulky end groups. However, the percent crystallinity of the polythiophene portion of the polymer remains approximately the same as that of the P3HT material. The powder X-ray scattering data indicate the presence of two distinct semicrystalline regimes in the C_{60}-P3HT-C_{60} polymer, which suggests that the end groups microphase separate from the main polymer chains to generate fullerene-rich and polythiophene-rich domains as was seen in a mixture of P3HT and C_{60}. The crystallite sizes of the P3HT domains were estimated to be on the order of 12 nm for both the P3HT and C_{60}-P3HT-C_{60} polymers using Scherrer's relation. Small-angle X-ray scattering showed that the characteristic domain spacings of the polymer powders were ~13 nm for both P3HT and C_{60}-P3HT-C_{60}. Finally, AFM phase images of thin films of the two polymers indicated that domain spacings consistent with SAXS data were also present in thin films of both of the polymer samples. The C_{60}-P3HT-C_{60} polymer behaves in a similar manner to the parent P3HT polymer in terms of light absorption, thermal properties, and microstructure. The covalent attachment of the fullerene to the polymer chain, which may enhance charge transfer, makes this new polymer a candidate for use as an electron-donating material in organic photovoltaics.

Acknowledgment. This work was funded by the Initiative for Renewable Energy and the Environment (IREE) at the University of Minnesota and the Xcel Renewable Development Fund. Parts of this work were carried out in the University of Minnesota IT Characterization Facility, which receives partial support from the NSF through the NNIN program. We thank Marc Rodwogin for help with prep SEC separation experiments and Benjamin D. Hamilton for help with WAXS experiments. We also thank Dr. Yang Qin and Derek M. Stevens for helpful discussions.

Supporting Information Available: Preparatory size exclusion chromatography (prep SEC), analytical SEC chromatograms for the polymers in chloroform over the entire elution volume range, matrix-assisted laser desorption/ionization−mass spectroscopy (MALDI-MS) spectra, elemental analysis results, and detailed synthetic procedures. This material is available free of charge via the Internet at http://pubs.acs.org.

References and Notes

(1) Sun, S., Sariciftci, N. S., Eds. *Organic Photovoltaics: Mechanisms, Materials, and Devices*; Taylor & Francis: Boca Raton, FL, 2005.
(2) Shaheen, S. E.; Ginley, D. S.; Jabbour, G. E. *MRS Bull.* **2005**, *30*, 10–15.
(3) Gunes, S.; Neugebauer, H.; Sariciftci, N. S. *Chem. Rev.* **2007**, *107*, 1324–1338.
(4) Li, G.; Shrotriya, V.; Huang, J.; Yao, Y.; Moriarty, T.; Emery, K.; Yang, Y. *Nat. Mater.* **2005**, *4*, 864–868.
(5) Ma, W.; Yang, C.; Gong, X.; Lee, K.; Heeger, A. J. *Adv. Funct. Mater.* **2005**, *15*, 1617–1622.
(6) Loewe, R. S.; Khersonsky, S. M.; McCullough, R. D. *Adv. Mater.* **1999**, *11*, 250–253.
(7) Chen, T.-A.; Wu, X.; Rieke, R. D. *J. Am. Chem. Soc.* **1995**, *117*, 233–244.
(8) Skotheim, T., Reynolds, J., Elsembauer, R., Eds. *Handbook of Conducting Polymers*; Marcel Dekker: New York, 1998.
(9) Osaka, I.; McCullough, R. D. *Acc. Chem. Res.* **2008**, *41*, 1202–1214.
(10) Nalwa, H. S., Ed. *Handbook of Organic Conductive Molecules and Polymers*; J. Wiley & Sons: New York, 1996.
(11) McCullough, R. D. *Adv. Mater.* **1998**, *10*, 93–116.
(12) Schilinsky, P.; Waldauf, C.; Brabec, C. J. *Appl. Phys. Lett.* **2002**, *81*, 3885–3887.
(13) Padinger, F.; Rittberger, R. S.; Sariciftci, N. S. *Adv. Funct. Mater.* **2003**, *13*, 85–88.
(14) Janssen, R. A. J.; Hummelen, J. C.; Sariciftci, N. S. *MRS Bull.* **2005**, *30*, 33–36.
(15) Thompson, B. C.; Fréchet, J. M. J. *Angew. Chem., Int. Ed.* **2008**, *47*, 58–77.
(16) Chirvase, D.; Parisi, J.; Hummelen, J. C.; Dyakonov, V. *Nanotechnology* **2004**, *15*, 1317–1323.
(17) Nguyen, L. H.; Hoppe, H.; Erb, T.; Gunes, S.; Gobsch, G.; Sariciftci, N. S. *Adv. Funct. Mater.* **2007**, *17*, 1071–1078.
(18) Muller, C.; Ferenczi, T. A. M.; Campoy-Quiles, M.; Frost, J. M.; Bradley, D. D. C.; Smith, P.; Stingelin-Stutzmann, N.; Nelson, J. *Adv. Mater.* **2008**, *20*, 3510–3515.
(19) Campoy-Quiles, M.; Ferenczi, T.; Agostinelli, T.; Etchegoin, P. G.; Kim, Y.; Anthopoulos, T. D.; Stavrinou, P. N.; Bradley, D. D. C.; Nelson, J. *Nat. Mater.* **2008**, *7*, 158–164.
(20) Xin, H.; Ren, G.; Kim, F. S.; Jenekhe, S. A. *Chem. Mater.* **2008**, *20*, 6199–6207.
(21) Bates, F. S.; Fredrickson, G. H. *Annu. Rev. Phys. Chem.* **1990**, *41*, 525–557.
(22) Russell, T. P.; Coulon, G.; Deline, V. R.; Miller, D. C. *Macromolecules* **1989**, *22*, 4600–4606.
(23) Morkved, T. L.; Lu, M.; Urbas, A. M.; Ehrichs, E. E.; Jaeger, H. M.; Mansky, P.; Russell, T. P. *Science* **1996**, *273*, 931–933.
(24) Hadziioannou, G. *MRS Bull.* **2002**, *27*, 456–460.
(25) Roncali, J. *Chem. Soc. Rev.* **2005**, *34*, 483–495.
(26) Cravino, A. *Polym. Int.* **2007**, *56*, 943–956.
(27) van Hall, P. A.; Knol, J.; Langeveld-Voss, B. M. W.; Meskers, S. C. J.; Hummelen, J. C.; Janssen, R. A. J. *J. Phys. Chem. A* **2000**, *104*, 5974–5988.
(28) Narutaki, M.; Takimiya, K.; Otsubo, T.; Harima, Y.; Zhang, H.; Araki, Y.; Ito, O. *J. Org. Chem.* **2006**, *71*, 1761–1768.
(29) Fernández, G.; Sánchez, L.; Veldman, D.; Wienk, M. M.; Atienza, C.; Guldi, D. M.; Janssen, R. A. J.; Martín, N. *J. Org. Chem.* **2008**, *73*, 3189–3196.
(30) Baffreau, J.; Ordronneau, L.; Leroy-Lhez, S.; Hudhomme, P. *J. Org. Chem.* **2008**, *73*, 6142–6147.
(31) Li, W.-S.; Yamamoto, Y.; Fukushima, T.; Saeki, A.; Seki, S.; Tagawa, S.; Masunaga, H.; Sasaki, S.; Takata, M.; Aida, T. *J. Am. Chem. Soc.* **2008**, *130*, 8886–8887.
(32) Ouhib, F.; Khoukh, A.; Ledeuil, J.-B.; Martinez, H.; Desbrières, J.; Dagron-Lartigau, C. *Macromolecules* **2008**, *41*, 9736–9743.
(33) Stalmach, U.; de Boer, B.; Videlot, C.; van Hutten, P. F.; Hadziioannou, G. *J. Am. Chem. Soc.* **2000**, *122*, 5464–5472.
(34) de Boer, B.; Stalmach, U.; van Hutten, P. F.; Melzer, C.; Krasnikov, V. V.; Hadziioannou, G. *Polymer* **2001**, *42*, 9097–9109.
(35) Richard, F.; Brochon, C.; Leclerc, N.; Eckhardt, D.; Heiser, T.; Hadziioannou, G. *Macromol. Rapid Commun.* **2008**, *29*, 885–891.
(36) Marcos-Ramos, A.; Rispens, M. T.; van Duren, J. K. J.; Hummelen, J. C.; Janssen, R. A. J. *J. Am. Chem. Soc.* **2001**, *123*, 6714–6715.
(37) Sivula, K.; Ball, Z. T.; Watanabe, N.; Fréchet, J. M. J. *Adv. Mater.* **2006**, *18*, 206–210.
(38) Sykes, A. G., Ed. *Advances in Inorganic Chemistry*; Academic Press: New York, 1996; Vol. *44*.
(39) Moriyama, H.; Kobayashi, H.; Kobayashi, A.; Watanabe, T. *J. Am. Chem. Soc.* **1993**, *115*, 1187–1189.
(40) Davey, S. N.; Leigh, D. A.; Moody, A. E.; Tetler, L. W.; Wade, F. A. *J. Chem. Soc., Chem. Commun.* **1994**, 397–398.
(41) Yamamoto, T.; Oguro, D.; Kubota, K. *Macromolecules* **1996**, *29*, 1833–1835.
(42) de Koning, G. J. M.; Lemstra, P. J. *Polymer* **1993**, *34*, 4089–4094.
(43) Lewis, J. E.; Maroncelli, M. *Chem. Phys. Lett.* **1998**, *282*, 197–203.
(44) Loewe, R. S.; Ewbank, P. C.; Liu, J.; Zhai, L.; McCullough, R. D. *Macromolecules* **2001**, *34*, 4324–4333.

(45) Trznadel, M.; Pron, A.; Zagorska, M.; Chrzaszcz, R.; Pielichowski, J. *Macromolecules* **1998**, *31*, 5051–5058.
(46) Sauvé, G.; McCullough, R. D. *Adv. Mater.* **2007**, *19*, 1822–1825.
(47) Dai, C.-A.; Yen, W.-C.; Lee, Y.-H.; Ho, C.-C.; Su, W.-F. *J. Am. Chem. Soc.* **2007**, *129*, 11036–11038.
(48) Boudouris, B. W.; Frisbie, C. D.; Hillmyer, M. A. *Macromolecules* **2008**, *41*, 67–75.
(49) Liu, J.; McCullough, R. D. *Macromolecules* **2002**, *35*, 9882–9889.
(50) Witiak, D. T.; Williams, D. R.; Kakodkar, S. V. *J. Org. Chem.* **1974**, *39*, 1242–1247.
(51) Maggini, M.; Scorrano, G.; Prato, M. *J. Am. Chem. Soc.* **1993**, *115*, 9798–9799.
(52) See Supporting Information for detailed synthetic procedures.
(53) El-Sayed, I.; Hazell, R. G.; Madsen, J. Q.; Norrby, P.-O.; Senning, A. *Eur. J. Org. Chem.* **2003**, *5*, 813–815.
(54) Elandaloussi, E. H.; Frère, P.; Richomme, P.; Orduna, J.; Garin, J.; Roncali, J. *J. Am. Chem. Soc.* **1997**, *119*, 10774–10784.
(55) Fazio, M. A.; Lee, P. O.; Shuster, D. I. *Org. Lett.* **2008**, *10*, 4979–4982.
(56) Ballenweg, S.; Gleiter, R.; Kratschmer, W. *Synth. Met.* **1996**, *77*, 209–212.
(57) Baffreau, J.; Ordronneau, L.; Lhez-Leroy, S.; Hudhomme, P. *J. Org. Chem.* **2008**, *73*, 6142–6147.
(58) Lambert, J. B.; Shurvell, H. F.; Lightner, D. A.; Cooks, R. G. *Organic Structural Spectroscopy*; Prentice Hall: Upper Saddle River, NJ, 1998.
(59) Yamashiro, T.; Aso, Y.; Otsubo, T.; Tang, H.; Harima, Y.; Yamashita, K. *Chem. Lett.* **1999**, 443–444.
(60) Fujitsuka, M.; Ito, O.; Yamashiro, T.; Aso, Y.; Otsubo, T. *J. Phys. Chem. A* **2000**, *104*, 4876–4881.
(61) Fujitsuka, M.; Matsumoto, K.; Ito, O.; Yamashiro, T.; Aso, Y.; Otsubo, T. *Res. Chem. Intermed.* **2001**, *27*, 73–88.
(62) Heiny, P. A.; Fischer, J. E.; McGhie, A. R.; Romanow, W. J.; Denenstein, A. M.; McCauley, J. P.Jr.; Smith, A. B.III; Cox, D. E. *Phys. Rev. Lett.* **1991**, *66*, 2911–2914.
(63) Liu, S. L.; Chung, T. S. *Polymer* **2000**, *41*, 2781–2793.
(64) Sperling, L. H. *Introduction to Polymer Science*, 3rd ed.; John Wiley & Sons: Hoboken, NJ, 2001.
(65) Malik, S.; Nandi, A. K. *J. Polym. Sci., Part B* **2002**, *40*, 2073–2085.
(66) Causin, V.; Marega, C.; Marigo, A.; Valentini, L.; Kenny, J. M. *Macromolecules* **2005**, *38*, 409–415.
(67) Cagiao, M. E.; Pozdnyakov, A. O.; Krumova, M.; Kudryavtsev, V. V.; Balta Callejà, F. J. *Compos. Sci. Technol.* **2007**, *67*, 2175–2182.
(68) Li, J. Q.; Zhao, Z. X.; Li, Y. L.; Zhu, D. B.; Gan, Z. Z.; Yin, D. L. *Physica C* **1992**, *196*, 135–140.
(69) Cullity, B. D. *Elements of X-Ray Diffraction*, 2nd ed.; Addison-Wesley Publishing Co.: Reading, MA, 1978.
(70) Erb, T.; Zhokhavets, U.; Gobsch, G.; Raleva, S.; Stuhn, B.; Schilinsky, P.; Waldauf, C.; Brabec, C. J. *Adv. Funct. Mater.* **2005**, *15*, 1193–1196.
(71) Moulé, A. J.; Meerholz, K. *Adv. Mater.* **2008**, *20*, 240–245.
(72) Zhong, H.; Yang, X.; deWith, B.; Loos, J. *Macromolecules* **2006**, *39*, 218–223.
(73) Zhang, R.; Li, B.; Iovu, M. C.; Jeffries-EL, M.; Sauve, G.; Cooper, J.; Jia, S.; Tristram-Nagle, S.; Smilgies, D. M.; Lambeth, D. N.; McCullough, R. D.; Kowalewski, T. *J. Am. Chem. Soc.* **2006**, *128*, 3480–3481.
(74) Liu, J.; Sheina, E.; Kowalewski, T.; McCullough, R. D. *Angew. Chem., Int. Ed.* **2002**, *41*, 329–332.